JBC RESEARCH ARTICLE

PvdM of fluorescent pseudomonads is required for the oxidation of ferribactin by PvdP in periplasmic pyoverdine maturation

Received for publication, March 11, 2022, and in revised form, June 21, 2022 Published, Papers in Press, June 25, 2022,
https://doi.org/10.1016/j.jbc.2022.102201

Michael-Frederick Sugue[1], **Ali Nazmi Burdur**[1], **Michael T. Ringel**[1], **Gerald Dräger**[2], **and Thomas Brüser**[1,*]
From the [1]*Institute of Microbiology, and* [2]*Institute of Organic Chemistry, Leibniz University Hannover, Hannover, Germany*

Edited by Donita Brady

Fluorescent pseudomonads such as *Pseudomonas aeruginosa* or *Pseudomonas fluorescens* produce pyoverdine siderophores that ensure iron-supply in iron-limited environments. After its synthesis in the cytoplasm, the nonfluorescent pyoverdine precursor ferribactin is exported into the periplasm, where the enzymes PvdQ, PvdP, PvdO, PvdN, and PtaA are responsible for fluorophore maturation and tailoring steps. While the roles of all these enzymes are clear, little is known about the role of PvdM, a human renal dipeptidase–related protein that is predicted to be periplasmic and that is essential for pyoverdine biogenesis. Here, we reveal the subcellular localization and functional role of PvdM. Using the model organism *P. fluorescens*, we show that PvdM is anchored to the periplasmic side of the cytoplasmic membrane, where it is indispensable for the activity of the tyrosinase PvdP. While PvdM does not share the metallopeptidase function of renal dipeptidase, it still has the corresponding peptide-binding site. The substrate of PvdP, deacylated ferribactin, is secreted by a Δ*pvdM* mutant strain, indicating that PvdM prevents loss of this periplasmic biosynthesis intermediate into the medium by ensuring the efficient transfer of ferribactin to PvdP *in vivo*. We propose that PvdM belongs to a new dipeptidase-related protein subfamily with inactivated Zn^{2+} coordination sites, members of which are usually genetically linked to TonB-dependent uptake systems and often associated with periplasmic FAD-dependent oxidoreductases related to D-amino acid oxidases. We suggest that these proteins are necessary for selective binding, exposure, or transfer of specific D- and L-amino acid–containing peptides and other periplasmic biomolecules in manifold pathways.

Iron is an essential element for many processes of life, such as cell metabolism, respirations, repair of DNA, and synthesis of proteins (1–4). Although iron is one of the most abundant elements in nature, it is hardly bioavailable under oxic conditions that result in poorly soluble Fe^{3+} hydroxides (5). In order to ensure sufficient iron supply for life-sustaining processes under iron-limiting conditions, many microorganisms produce so-called siderophores, small iron-chelating compounds that are released into the environment and taken up together with bound iron. Especially, host environments are such iron-limiting habitats, and therefore, siderophore production has been found to play an important role for the virulence of pathogenic bacteria as well as for the beneficial function of mutualistic symbioses (6, 7). These iron-binding chelators enable the specific binding and dissolving of Fe^{3+} from compounds in the habitat and the uptake of iron into the cell. One of these siderophores is pyoverdine, which is formed by a number of different fluorescent pseudomonads, such as *Pseudomonas aeruginosa* or *Pseudomonas fluorescens*. Pyoverdines play an important role not only for iron supply but also for signaling that results in the production of virulence factors (8). More than 100 different variants of pyoverdines are known to date, which all share three characteristic features that had been identified first in pyoverdine from *P. aeruginosa* (9). They all have an invariable hydroxyquinoline core that is responsible for the characteristic fluorescence of pyoverdine, and they have a peptide backbone of partly unusual D- and L-amino acids, which can vary in length and composition between species and even strains. Furthermore, they possess a variable side chain at their fluorophore, which results from various possible modifications of the N-terminal glutamate that is always present in the ferribactin precursor (10). While nonribosomal synthesis of ferribactin takes place in the cytoplasm, the maturation of pyoverdine by the enzymes PvdQ, PvdP, PvdO, PvdN, and PtaA is a periplasmic process. The roles of these enzymes have been identified, and since then, enzymes are known for all maturation reactions (11–13). However, one further protein, PvdM, is known to be essential for pyoverdine biosynthesis, but its exact role remained a mystery until now.

Here, we reveal the function of this last essential pyoverdine biogenesis protein. We describe biochemical and physiological studies on PvdM that demonstrate that this protein is required inside the periplasm, where it is necessary for the oxidation of ferribactin by PvdP *in vivo*. Without PvdM, ferribactin is lost from the periplasm and not available as substrate for PvdP.

Results

PvdM is a membrane-anchored protein facing the periplasm

PvdM has been shown to be essential for biosynthesis of pyoverdines, but its function within this pathway has remained

* For correspondence: Thomas Brüser, brueser@ifmb.uni-hannover.de.

a mystery (13). PvdM is structurally related to M19 peptidases, which are membrane dipeptidases like human renal dipeptidase (hrDP, (14, 15)). For this reason, PvdM has been tentatively assigned as dipeptidase or putative dipeptidase in proteomes of the sequenced *Pseudomonas* strains (16). However, enzymes have been identified for all known reactions of pyoverdine biosynthesis (10), and no obvious function remained for PvdM. Working on this question, we first narrowed down potential roles by determining the subcellular localization of PvdM. The N-terminus of PvdM resembles a signal peptide, with a positively charged n-region and a hydrophobic h-region (Fig. 1*A*). However, this hydrophobic region is sufficiently long to serve as transmembrane helix (21 residues) and terminates with a strictly conserved tryptophan (Trp-29), which is a typical residue for the border region of transmembrane helices in membrane proteins (17). At the beginning of this study, we therefore hypothesized that the C-terminal domain should be anchored to the periplasmic face of the cytoplasmic membrane by an N-terminal transmembrane domain, and PvdM would therefore function somewhere in periplasmic maturation steps.

To address this aspect, we analyzed the subcellular localization of PvdM in our nonpathogenic model organism *P. fluorescens* A506, which uses the same periplasmic pathway for pyoverdine maturation as other fluorescent pseudomonads, such as the pathogen *P. aeruginosa*. Beside the wildtype PvdM, we also analyzed two variants that either possessed an engineered signal peptidase cleavage site or a *bona fide* signal peptide at the N-terminus (Fig. 1*A*). Wildtype PvdM was exclusively found in the membrane fraction, suggesting that the N-terminal transmembrane domain anchors the globular C-terminal domain to the membrane (Fig. 1*B*). In case of the PvdM variant with the engineered signal peptidase cleavage site, PvdM(ASA), the N-terminal membrane anchor was cleaved off, as expected, but the total protein abundance was markedly decreased, suggesting that a PvdM that lacks residues Met-1 to Trp-29 is highly protease sensitive. The cleaved protein, however, was still in the membrane and remained membrane bound in carbonate washes, indicating that there must exist an additional membrane anchor, possibly some lipidation as known for the related hrDP (18). As Trp-29 at the end of the transmembrane helix of PvdM is strictly conserved in PvdM, we thought that the removal of the C-terminal region of the transmembrane helix in the PvdM(ASA) construct might cause the observed destabilization. Therefore, we constructed a PvdM variant, named PvdOsp–PvdM, in which only residues 1 to 24 were exchanged by the proper Sec signal peptide of PvdO (13) (Fig. 1*A*). In this case, cleavage should result in a mature PvdM with the last five residues of the transmembrane helix remaining at its N-terminus. As expected, this construct was processed, and, more importantly, the protein was stable, which indicates that the last residues of the transmembrane helix are indeed important for stability of PvdM (Fig. 1*B*). As in the case of PvdM(ASA), PvdOsp–PvdM also resulted in membrane-associated PvdM that was resistant to carbonate washes, indicating that there must exist a membrane anchor in addition to the transmembrane helix that had been cleaved off in these constructs. As signal peptidase is active on the periplasmic face of the cytoplasmic membrane, cleavage of the two constructs indicated a periplasmic localization of the cleavage site, suggesting transport of the C-terminal domain into the periplasm. Direct comparison of PvdM and the two signal peptide variants by SDS-PAGE/Western blotting of membrane fractions clearly confirmed signal peptide cleavage of the signal peptides and the lowered abundance in case of the construct PvdM(ASA) (Fig. 1*C*). The engineered cleaved signal peptides contained cleavage sites that were predicted to function with 90% and 95% probability, as judged by SignalP 5.0 (19), whereas the noncleaved membrane anchor had no likely cleavage site (<7%, Fig. 1*D*).

As signal peptide cleavage of the PvdM(ASA) and PvdOsp–PvdM constructs had not resulted in a release of mature PvdM into the periplasm, we substituted the globular C-terminal domain of PvdM by the mature domain of *Escherichia coli* alkaline phosphatase (PvdMnt-PhoA) and analyzed PhoA-transport and activity to examine whether the membrane anchor of PvdM enables transport of C-terminal domains into the periplasm (Fig. 2*A*). Being only active in the periplasm, PhoA activity is a marker for successful transport into this compartment (20). As negative controls, we measured PhoA activity in an empty vector control strain as well as in a strain that produces mature PhoA that lacks a signal peptide and therefore cannot be transported into the periplasm. As positive controls, we measured PhoA activity in a strain that produced a PhoA fused to the signal peptide of PvdO and in a strain that produced the PhoA precursor with its natural signal peptide (prePhoA). As a result, we clearly observed PhoA activity in the PvdMnt-PhoA fusion, indicating that the membrane anchor of PvdM directs C-terminal domains into the periplasm. The two positive controls were positive, and the two negative controls were negative.

Subcellular fractionations revealed that the PvdO signal peptide had resulted in soluble PhoA in the periplasmic fraction, indicating correct functioning of this signal peptide (Fig. 2*B*). As observed already with PvdM, the PvdMnt-PhoA fusion resulted in membrane-bound PhoA, confirming the aforementioned observation that the N-terminal hydrophobic region of PvdM represents a noncleaved transmembrane domain.

To examine the periplasmic exposure of the membrane-anchored globular domain by another independent method, we carried out a protease accessibility assay. For this experiment, we produced PvdM in *E. coli* BL21 (DE3), whose outer membrane can be readily permeabilized for proteases by EDTA treatment (21). We thus permeabilized outer membranes by EDTA treatment and degraded periplasmically exposed protein domains by proteinase K (Fig. 2*C*). Notably, PvdM was readily degraded, whereas the cytoplasmic biotin carboxyl carrier protein (BCCP) was not, indicating a periplasmic localization of PvdM. As a control, an addition of detergent to the cells, which permeabilizes the cytoplasmic membrane, resulted in complete degradation also of the cytoplasmic BCCP.

Together, the signal peptidase cleavage of the PvdM(ASA) and PvdOsp–PvdM constructs, the transport of fused PhoA of

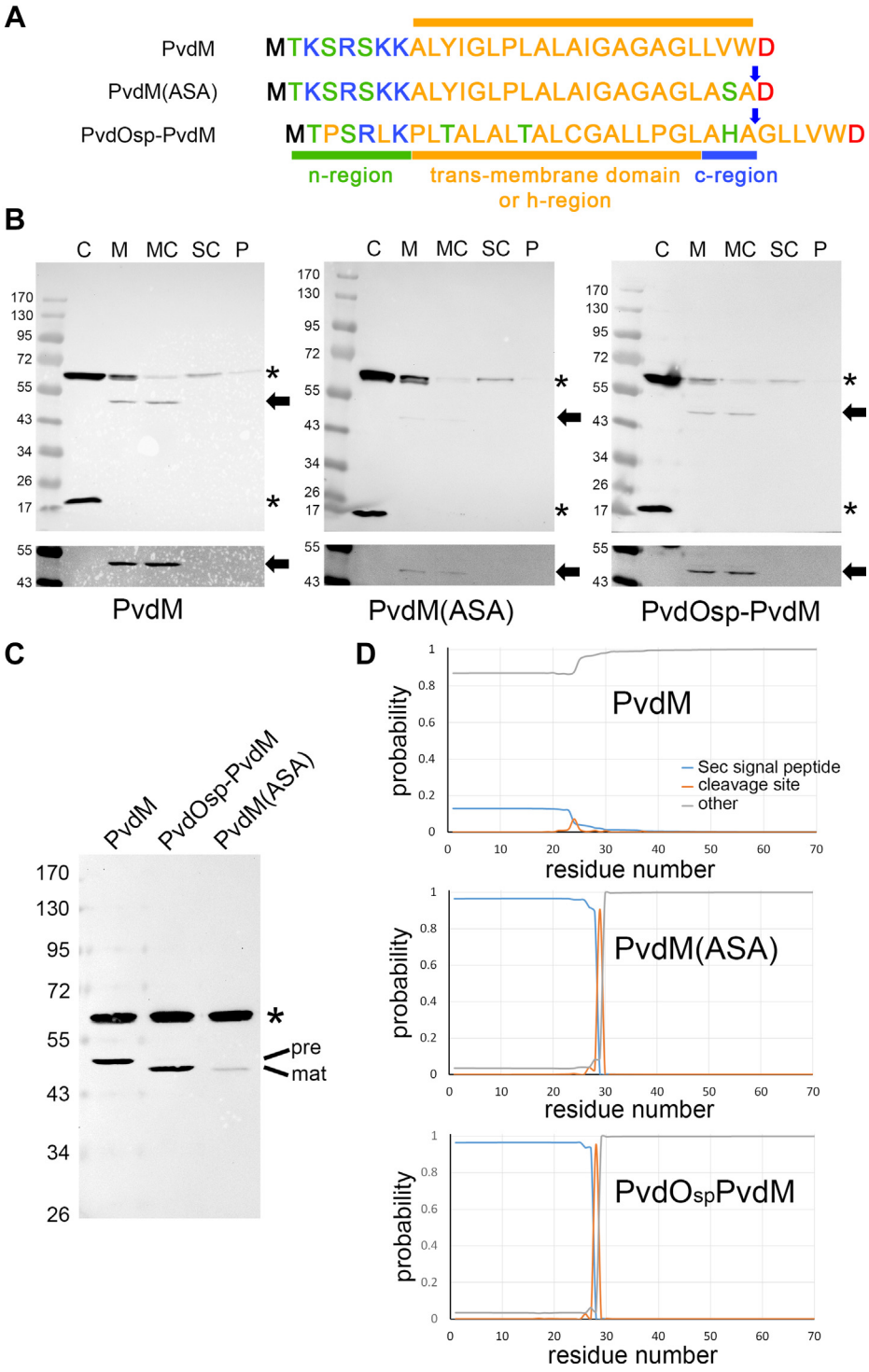

Figure 1. The N-terminus of PvdM is a membrane anchor. *A*, comparison of the three constructs used to analyze the N-terminal transmembrane domain of PvdM in *Pseudomonas fluorescens* A506. The regions corresponding to signal peptide n-, h-, and c-regions and the signal peptide cleavage sites (*arrows*) are indicated. *B*, subcellular localization analyses of the three tested PvdM constructs as produced in *P. fluorescens* A506 Δ*pvdM* using pUCP20-ANT2-His-*pvdM*-strep-term, pUCP20-ANT2-His-*pvdM*-ASA-strep-term, pUCP20-ANT2-His-SP-*pvdO*-mat-*pvdM*-strep-term, and detected by use of their C-terminal *Strep*-tags. Cytoplasmic (C), membrane (M), and periplasmic (P) fractions of the indicated strains were analyzed by SDS-PAGE/Western blotting for the presence of PvdM. In addition, the membrane fractions were carbonate washed, and the membranes after carbonate wash (MC) as well as the supernatant after carbonate wash (SC) were included in the analyses. The *arrow* indicates the position of PvdM. *Asterisks* indicate positions of nonspecific crossreactions. Molecular weight markers (kilodalton) are indicated on the *left*. Equally enhanced regions of the full blots are added to visualize the weak PvdM bands of the PvdM(ASA) construct. Note that, in all cases, PvdM remained membrane-bound even after carbonate washes. *C*, direct SDS-PAGE/Western blot comparison of these PvdM variants in membrane fractions, as detected by their C-terminal *Strep*-tags. Note that the two constructs with signal peptide cleavage sites were processed to mature form, whereas wildtype PvdM was not processed. *D*, prediction of signal peptidase cleavage sites by SignalP, indicating the absence of a cleavage site in wildtype PvdM, and a presence of cleavage sites in the two other constructs.

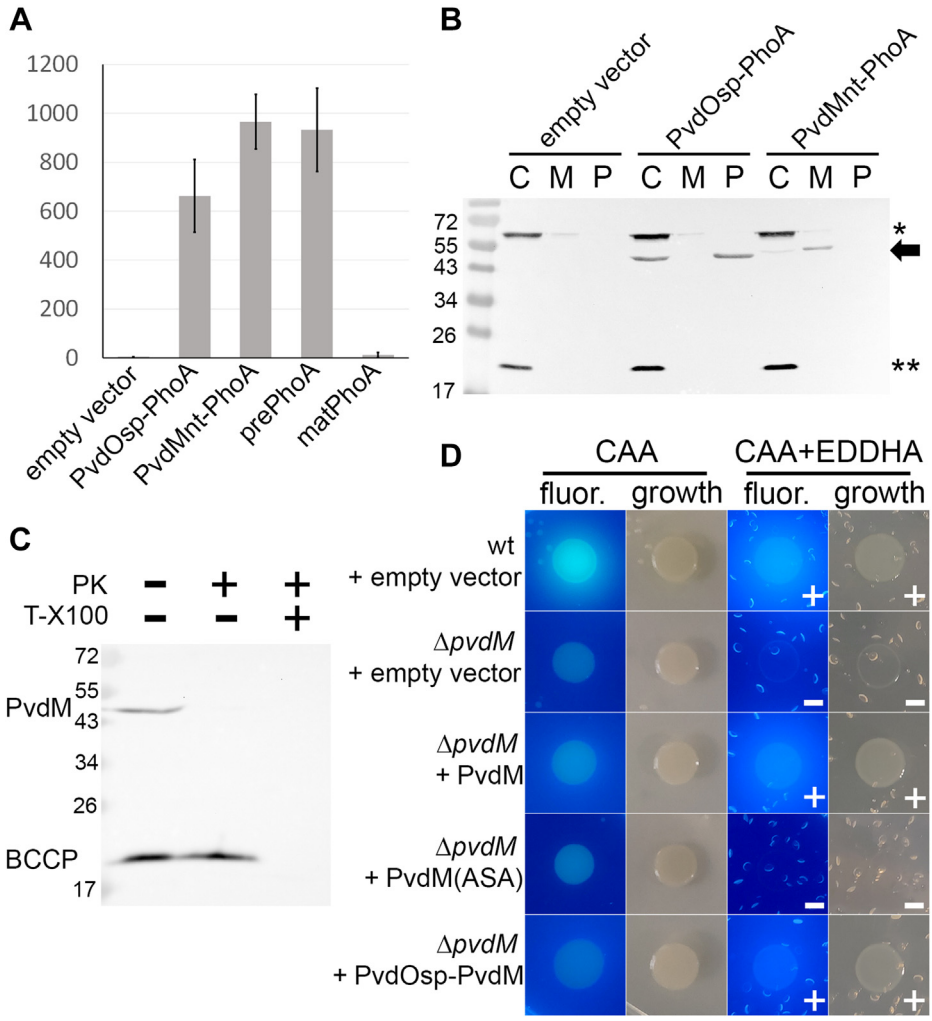

Figure 2. PvdM is functional on the periplasmic side of the cytoplasmic membrane. *A*, PhoA activity in *Pseudomonas fluorescens* A506 transformants producing the indicated proteins using the vectors pUCP20-ANT2-His-SP-*pvdO*-mat-*phoA*-strep-term, pUCP20-ANT2-His-SP-*pvdM*-mat-*phoA*-strep-term, pUCP20-ANT2-*phoA*-strep-term, and pUCP20-ANT2-mat-*phoA*-strep-term. pUCP20-ANT2-MCS is used as empty vector control. Note that signal peptides (constructs PvdOsp-PhoA and prePhoA) as well as the membrane anchor of PvdM (construct PvdMnt-PhoA) resulted in periplasmic PhoA activity, whereas the empty vector or the signal peptide–deficient mature PhoA (matPhoA) did not. *B*, signal peptides result in the secretion of PhoA into the periplasm, whereas the N-terminus of PvdM results in membrane-anchored PhoA in *P. fluorescens* A506. Detections of the PhoA constructs (C-terminal *Strep*-tags) in which the mature domain of PhoA was fused either to a cleavable signal peptide (PvdOsp-PhoA) or to the membrane anchor of PvdM (PvdMnt-PhoA). Cytoplasm (C), membrane (M), and periplasm (P) were analyzed by SDS-PAGE/Western blot analysis. The *arrow* indicates the position of PvdM. The *asterisks* indicate positions of two cytoplasmic biotin–containing proteins that are nonspecifically detected by the Strep-Tactin-HRP conjugate and can be taken as fractionation control. Note that most likely some periplasm contaminates the cytoplasmic fraction, as seen with the PvdOsp-PhoA construct, but this is not relevant for the detection of the transport. *C*, degradation of periplasmically exposed PvdM by proteinase K in outer membrane–permeabilized *Escherichia coli*. PvdM, produced using pEX-*pvdM*-strep-term-tac, is detected by SDS-PAGE/Western blotting (detection of C-terminal *Strep*-tag). Without proteinase K, PvdM and the cytoplasmic marker protein biotin carboxyl carrier protein (BCCP) are detectable (*left lane*). Proteinase K addition results in the selective degradation of PvdM (*middle lane*), and detergent addition (Triton X-100) causes complete degradation also of the cytoplasmic BCCP. Indicated marker positions are the same as in *B*. *D*, growth and fluorescence of indicated strains growing on iron-limiting CAA (*left*) and iron-depleted CAA + EDDHA (*right*) medium. PvdM is required for growth and fluorescence on CAA + EDDHA medium. Note that not only the wildtype strain and the PvdM-complemented Δ*pvdM* strain forms pyoverdine but also the strain with the PvdOsp–PvdM fusion construct. CAA, casamino acid; EDDHA, ethylene diamine-*N*,*N*′-bis(2-hydroxyphenylacetic acid); HRP, horseradish peroxidase; PhoA, alkaline phosphatase.

the PvdMnt-PhoA construct, and the protease accessibility experiment all indicated a periplasmic exposure of the globular domain of membrane-associated PvdM.

The N-terminus and most of the membrane anchor are not essential for activity of PvdM

We addressed the activity of wildtype PvdM and the two signal peptide–containing engineered variants by testing pyoverdine production and growth support on casamino acid (CAA) medium containing ethylene diamine-*N*,*N*′-bis(2-hydroxyphenylacetic acid) (EDDHA), which results in an iron limitation that only permits growth in case of functional pyoverdine production (11). We analyzed the *P. fluorescens* A506 wildtype strain with the empty vector (positive control), the Δ*pvdM* strain with the empty vector (negative control), the Δ*pvdM* strain with the *pvdM*-complementation vector (positive control), and Δ*pvdM* strains with complementation vectors for the two signal peptide–containing variants PvdM(ASA) and PvdOsp–PvdM (Fig. 2*D*). All these strains

were also grown on CAA medium without EDDHA to show their growth (positive control). As expected, the wildtype and the *pvdM*-complemented Δ*pvdM* strain did grow on EDDHA-containing medium, whereas the Δ*pvdM* strain with the empty vector did not, and all strains grew on plates without EDDHA. In case of the signal peptide–containing variants, we observed neither growth nor pyoverdine production on EDDHA-containing plates with the PvdM(ASA) variant, whereas we did observe growth and pyoverdine production with the PvdOsp–PvdM variant. As the PvdM(ASA) variant was significantly less abundant (Fig. 1*C*), we cannot say whether the removal of the transmembrane domain had specific functional effects in addition to the general destabilization. However, the function of the PvdOsp–PvdM variant clearly demonstrated that the N-terminal region up to position Ala24 is dispensable for activity. As the PvdOsp–PvdM and wildtype PvdM had comparable stabilities (Fig. 1*C*), it can be concluded that residues of the end of the transmembrane domain, that is, residues of the GLLVW sequence, are important for stability of the globular periplasmic domain of PvdM.

PvdM is not the unknown site 1-protease that cleaves FpvR

As PvdM is structurally related to renal dipeptidase, it is usually assigned as dipeptidase in genomic assignments. We asked the question how a periplasmic peptidase could be essential for pyoverdine biosynthesis. As there is no peptidase directly involved in pyoverdine maturation, it was possible that PvdM might be the unknown peptidase required for initial cleavage (site 1-like protease) of a periplasmic domain of FpvR, the antisigma factor that inhibits the activity of the sigma factors PvdS and FpvI (22). If PvdM was that protease, its absence would abolish the initial cleavage of FpvR, leading to a constant inhibition of pyoverdine biosynthesis, which could explain why there is no pyoverdine detectable without PvdM. To test this, we generated a double mutant strain deleted in *pvdM* and *fpvR*. As expected for an antisigma factor deletion, the *fpvR* deletion strain is known to constitutively express the pyoverdine biogenesis genes (8). If PvdM was the site 1-like proteases, this double mutant strain would rescue the Δ*pvdM* phenotype and show a constant pyoverdine production because of the absence of the antisigma factor. However, the double knockout strain *P. fluorescens* A506 Δ*fpvR*Δ*pvdM* was neither able to grow on CAA medium plates supplemented with EDDHA for iron depletion nor was this strain capable of producing pyoverdine under iron-limiting conditions (Fig. 3). Therefore, it was clear from this experiment that PvdM is not involved in this regulatory pathway of pyoverdine synthesis.

PvdM is required for the turnover of ferribactin by PvdP in vivo and prevents ferribactin secretion into the medium

As we have found that PvdM plays its essential role for pyoverdine biogenesis inside the periplasm, and as it is not involved in the regulatory activation of the FpvR-dependent signaling cascade, a potential role in the periplasmic pyoverdine maturation steps remained. To address this aspect

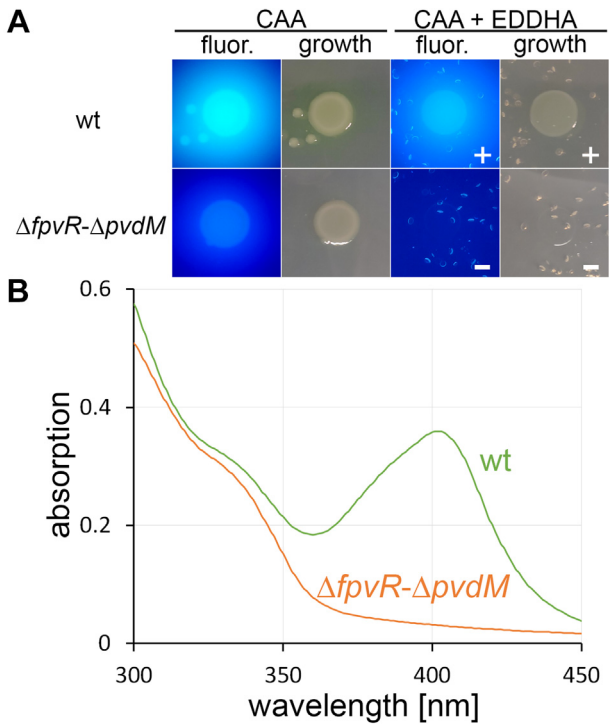

Figure 3. The deletion of the antisigma factor gene *fpvR* does not rescue the Δ*pvdM* phenotype. *A*, growth and pyoverdine production of a Δ*fpvR*-Δ*pvdM* mutant strain in comparison to the wildtype. Note that the double mutant does not produce pyoverdine and therefore does not grow on CAA + EDDHA medium. *B*, pyoverdine detection in liquid culture supernatants of the strains grown on CAA medium. Note that the wildtype strain produces pyoverdine, whereas the double mutant strain does not. CAA, casamino acid; EDDHA, ethylene diamine-*N*,*N*′-bis(2-hydroxyphenylacetic acid).

directly, we asked the question whether a certain non-fluorescent and hence so far not detected intermediate of the pyoverdine maturation accumulates in the Δ*pvdM* strain. We therefore searched in the medium of the Δ*pvdM* strain for potentially secreted biogenesis intermediates. Strikingly, we clearly detected deacylated ferribactin (exact mass = 1178.580 Da) as the only pyoverdine biogenesis pathway intermediate (Figs. 4*A* and S1). Deacylated ferribactin is known to be the substrate of PvdP. We thus carried out the same analysis with a Δ*pvdP* strain, and, as expected, we found the same intermediate. In the Δ*pvdM* strain, the ferribactin is therefore still deacylated by PvdQ but apparently not further oxidized by PvdP, demonstrating that PvdM is essential for the turnover of ferribactin by PvdP *in vivo*.

Ferribactin is often released in small amounts from pyoverdine-producing strains (12), and we consequently compared the quantities of ferribactin that is released into the medium by the Δ*pvdM* strain with the ferribactin that can be detected in the medium of the wildtype strain (Fig. 4*B*). Remarkably, in this assay, the deletion of Δ*pvdM* resulted in an over 35-fold increase of released ferribactin. Less than 3% ferribactin was found in the medium of the wildtype in comparison to the medium of the Δ*pvdM* strain, demonstrating that PvdM very efficiently prevented ferribactin release. These data indicate that there is only little deacylated ferribactin available for exporters in the presence of PvdM, which thus

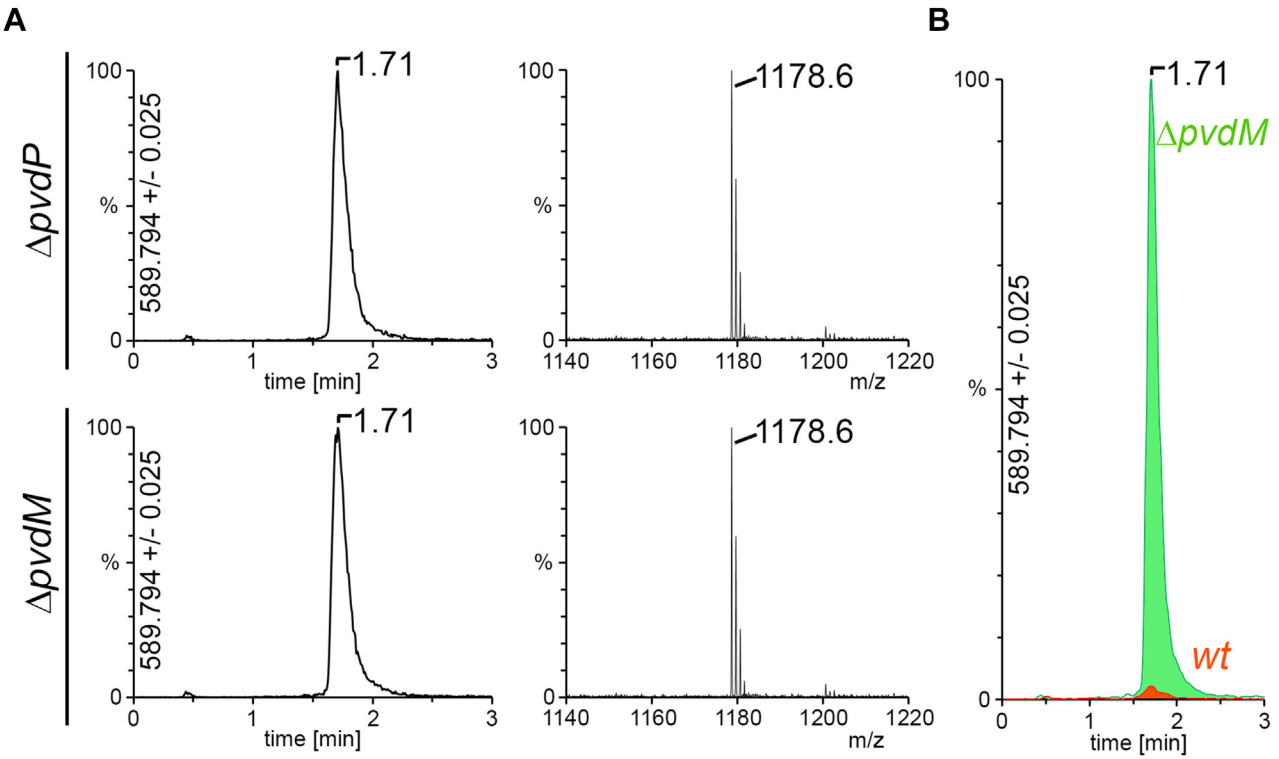

Figure 4. Deacylated ferribactin is secreted in the Δ*pvdM* mutant strain. *A*, analysis of pyoverdine content in culture supernatants of *Pseudomonas fluorescens* A506 Δ*pvdP* and Δ*pvdM* mutant strains. *Right*, mass spectra, showing the detection of deacylated ferribactin (mass: 1178.6) in the supernatant of both strains. The shown spectra integrate signals of 1.6 to 1.85 min retention time, covering all pyoverdine compounds. Extracted ion chromatograms of all possible pyoverdine-related compounds are available online (Fig. S1). Note the absence of any further pyoverdine-related compound. *Left*, elution profiles that monitor the respective molecular mass of the double-charged species during reverse-phase chromatography. *B*, direct comparison of ferribactin levels in the medium of the Δ*pvdM* mutant strain (*green*) and the wildtype strain (*red*), using elution profiles as in (*A*) after two times smoothing (window size = 2). Peak areas (arbitrary units) were 155 for Δ*pvdM* and 4.4 for the wildtype.

ensures—directly or indirectly—efficient transfer of the ferribactin to PvdP.

PvdM does not contain the dipeptidase zinc-binding site

PvdM is generally annotated as dipeptidase, which is due to sequence similarity to hrDP and related bacterial dipeptidases (23). However, the requirement of PvdM for the turnover of ferribactin by PvdP indicated that PvdM does not function as a dipeptidase, although it still likely binds a peptide, namely ferribactin. To address this aspect further, we analyzed the potential dipeptidase active site in PvdM. HrDP is a dimeric metalloprotease that coordinates two catalytic Zn^{2+} ions per subunit (14). His-20, Asp-22, and Glu-125 bind the first Zn^{2+}, and Glu-125, His-198, and His-219 bind the second Zn^{2+}. Glu-125 is bridging the two Zn^{2+} ions. His-20 and His-198 have been shown to be essential for activity (24), and also Glu-125 exchanges other than E125Q inactivate hrDP (25). Of these five ligands, only His-219 is strictly conserved in PvdM homologs. However, in direct vicinity of the His-198 ligand position, there is a strictly conserved methionine residue in the corresponding sequence of PvdM, which we thought might also serve as ligand for Zn^{2+}, although this would be an untypical ligand for Zn^{2+} (Fig. 5*A*). Therefore, PvdM contains two potential ligands for one metal-binding site that would correspond to the second Zn^{2+} ion site in hrDP, which are Met-246 and His-266 in *P. fluorescens* A506 PvdM (Fig. 5*A*). We tested the potentially important function of these two candidate ligands by alanine exchanges. The M246A exchange resulted in complete PvdM degradation and inactivity (Fig. 5*B*). It therefore is clear that the strictly conserved Met-246 is required for stability of PvdM. In contrast, the H266A exchange did not affect protein stability. In the growth assay, the strain with PvdM-M246A did not grow on CAA/EDDHA, whereas the strain with PvdM-H266A produced pyoverdine and therefore could grow (Fig. 5*B*). Since four of five zinc ligands are not conserved in *P. fluorescens* A506 PvdM, and as the only positionally conserved potential ligand, His-266, is irrelevant for PvdM function, we conclude that, in contrast to renal dipeptidase, there is no functional zinc site in PvdM. This was expected, as we had found that PvdM is only required for PvdP function and does not *per se* catalyze any reaction. The data also agree with a crystal structure of a soluble C-terminal domain of PvdM from a *P. aeruginosa* strain, heterologously produced in *E. coli* BL21 DE3, that has been uploaded in Protein Data Bank in 2007 without an accompanying publication (Protein Data Bank ID: 3B40). There is no zinc site in that structure, and the structure also shows that the aforementioned analyzed methionine is indeed pointing with its side chain toward the interior of the protein, which excludes a function as metal ligand and explains the observed importance for protein stability. The absence of the catalytic Zn^{2+}-binding

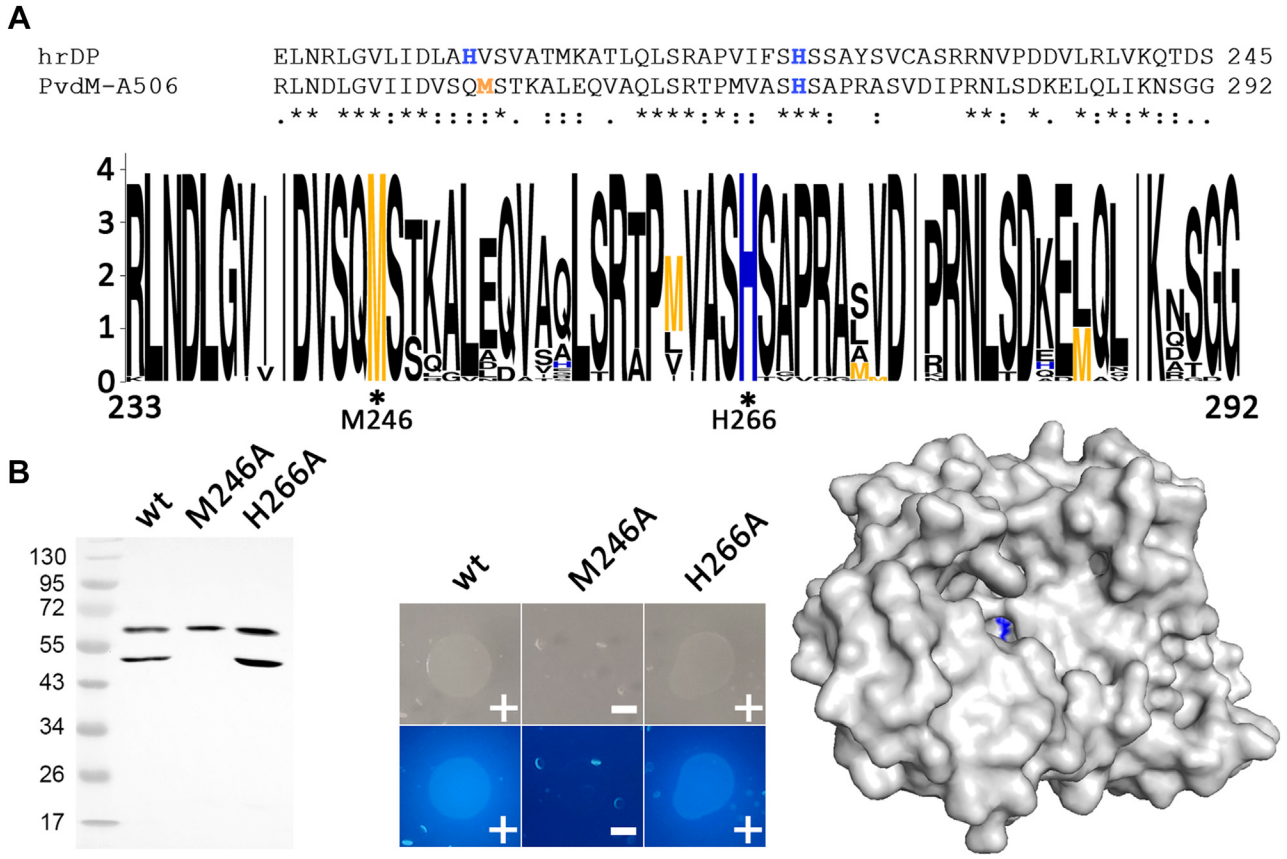

Figure 5. PvdM does not have the dipeptidase active site. *A*, sequence conservation between human renal dipeptidase and PvdM in the region of the potentially conserved zinc ligands (*upper alignment*) and conservation of residues of this region within PvdM sequences from 35 different *Pseudomonas* species (WebLogo plot, (43)). Histidines are highlighted in *blue*, and methionines are highlighted in *yellow*. The only conserved ligand from the binuclear hrDP Zn^{2+} site, His-266, and the conserved methionine that was also considered as potential ligand (Met-246), are indicated. *B*, analyses of the PvdM variants M246A and H266A (produced using pUCP20-ANT2-*pvdM*M246A-strep-term and pUCP20-ANT2-*pvdM*H266A-strep-term; detection by the C-terminal *Strep*-tag), in comparison to the wildtype. SDS-PAGE/Western blot analysis (*left*) and functional analysis (*middle*, see legend for Fig. 2 for details). The structure of PvdM from *P. fluorescens* A506 (*right*) has been homology modeled using Swiss Model (44), based on the structure from *P. aeruginosa* (Protein Data Bank ID: 3B40), and visualized using PyMOL (45). The His-266 deep in the peptide-binding pocket is highlighted in *blue*. hrDP, human renal dipeptidase.

site in PvdM indicates that PvdM is not a dipeptidase, although it has overall structural similarity to renal dipeptidase.

PvdM most likely requires the peptide-binding site of dipeptidase origin for function

The hrDP binds specific peptides and hydrolyzes them. While the responsible hydrolytic site is not conserved in PvdM, the peptide-binding ability is likely conserved. To examine whether the potential peptide-binding site is functionally important for PvdM, we tested whether the activity of PvdM is affected by cilastatin. Renal dipeptidase is competitively inhibited by cilastatin, which occupies the peptide-binding active site (26), and we considered that a conservation of this binding site in PvdM might permit inhibition of PvdM activity by cilastatin. The structure of renal dipeptidase with bound cilastatin is known (14), and the binding region is quite conserved in PvdM, including three of four side chains of renal dipeptidase that are responsible for hydrogen bonding to cilastatin, accounting for five of six hydrogen bonds (Fig. 6*A*). We therefore cultivated the wildtype strain *P. fluorescens* A506 containing the empty vector, the Δ*pvdM* strain containing the empty vector, and the Δ*pvdM* strain containing the complementation vector in CAA/EDDHA medium with or without cilastatin (Fig. 6*A*). In agreement with the data obtained with solid media (Fig. 2), the non-complemented Δ*pvdM* strain did not grow. The wildtype strain grew better than the complementation strain, indicating that complementation was not complete but sufficient to support growth. Importantly, in both cases, growth of the wildtype or complemented strain was clearly inhibited by cilastatin, which apparently could enter the periplasm and interact with PvdM. In controls without iron limitation, cilastatin had no significant effect on growth. As cilastatin binds competitively and highly specific to the peptide-binding site of hrDP, and as important cilastatin-binding residues are conserved in PvdM, we would like to carefully conclude that our results are a first evidence for a role of this peptide-binding site in PvdM, which appears to be important for the function of PvdP *in vivo*.

PvdP is a tyrosinase and requires copper assembly to its type-3-copper site for activity. *In vitro*, copper can assemble

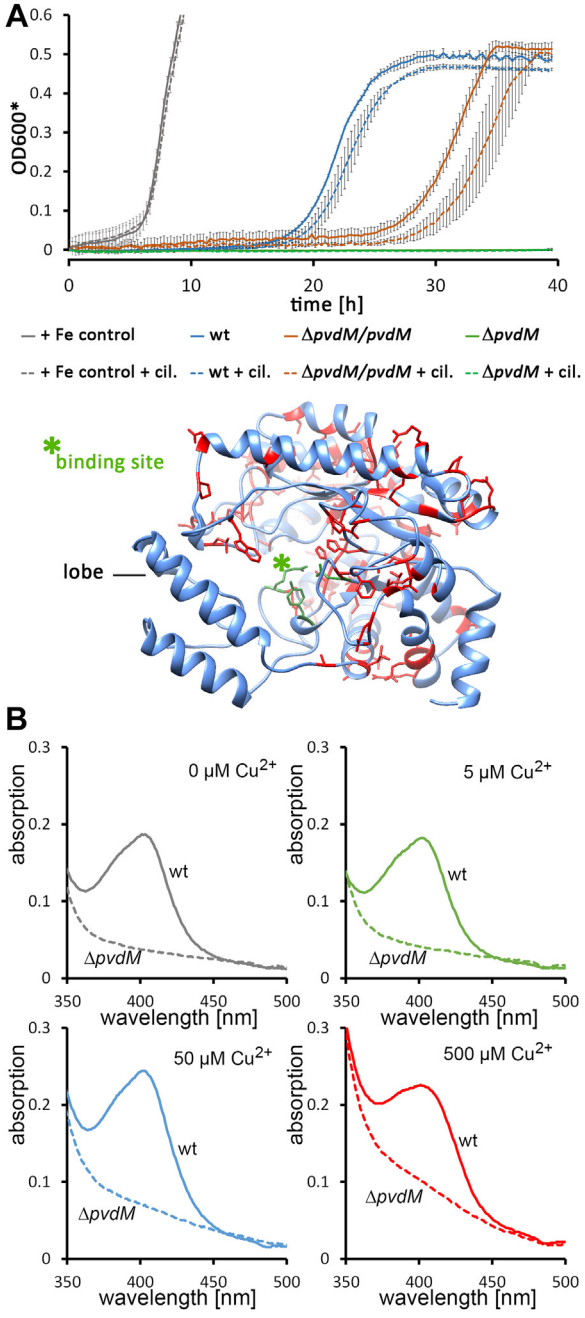

Figure 6. A conserved peptide-binding site of PvdM is likely to be important for function. *A*, *upper part*, growth of *Pseudomonas fluorescens* A506 (wt), its *pvdM*-complemented Δ*pvdM* mutant (Δ*pvdM/pvdM*), and the not complemented Δ*pvdM* mutant in CAA + EDDHA medium with or without 1 mM cilastatin. The onset of growth of the Δ*pvdM/pvdM* strain in this medium in the presence of 100 μM $FeCl_3$ is included as control (+Fe control), showing that there is no growth delay under iron-repleted conditions (growth continues to an absorbance of ∼1 at 600 nm; *initial path length: 5.3 mm). Note that cilastatin results in a significant growth inhibition of the wildtype and the complemented mutant strain. The non-complemented mutant strain cannot grow on this iron-depleted medium (Fig. 2). Error bars are from technical triplicates. *A*, *lower part*, position of conserved renal dipeptidase residues in PvdM from *P. fluorescens* A506 (Fig. 5). Identical residues are highlighted in *red* and *green*, with the cilastatin-binding residues R277, Y302, and D391 in *green* (corresponding to R230, Y255, and D288 in renal dipeptidase (14)). A new structural lobe that is found in PvdM but not in renal dipeptidase is also indicated (see text for details). *B*, addition of copper does not compensate for the absence of PvdM in a Δ*pvdM* mutant. Pyoverdine production is monitored by electronic absorption spectroscopy. Media contained 0, 5, 50, or 500 μM $CuSO_4$, as indicated. Note that even at 500 μM copper, which is beginning to become toxic to the cells, no pyoverdine can be formed without PvdM, indicating that copper limitation plays no role in the PvdM phenotype. CAA, casamino acid; EDDHA, ethylene diamine-*N*,*N*′-bis(2-hydroxyphenylacetic acid).

spontaneously to PvdP in the presence of substrate (27, 28). The substrate peptide displaces a tyrosine at the active site, which results in a remodeling of PvdP and spontaneous copper assembly, most likely facilitated by two methionines near the copper site (28). Without PvdM, we found that no pyoverdine was produced, even in media with very high copper concentrations that suffice to activate PvdP *in vitro* in the presence of substrate (Fig. 6*B*, (27, 28)), indicating that it is not any copper limitation but rather substrate access that requires PvdM *in vivo*.

PvdM appears to be the first member of a novel nonhydrolytic protein family structurally related to dipeptidases, which likely is involved in specific recognition and transfer of peptides and other biomolecules

As PvdM plays an essential role for pyoverdine biogenesis, we asked the question whether homologs of PvdM exist that may play similar roles in different pathways of other bacteria. Such homologs might prevent loss of biomolecules from the periplasm or ensure their efficient transfer to enzymes in biosynthetic or degradation pathways. To find such PvdM-related proteins, we searched for PvdM homologs in proteobacteria by BlastP analyses (29) and excluded the order Pseudomonadales from this search. Among the top 100 hits, 46 hits came from whole-genome analyses, and we focused on these in order to be able to examine the genomic background. We only found PvdM homologs in the α-, β-, and γ-proteobacteria, not in the δ- and ε-proteobacteria. Among these, five hits came from PvdM homologs that had neither a signal peptide nor an N-terminal transmembrane domain, as predicted by SignalP 5.0 or TMHMM 2.0 (19, 30), and therefore, these hits were unlikely to be periplasmic. The other 41 hits were thus predicted periplasmic PvdM homologs with or without membrane anchor. All of them had at least the key bridging ligand substituted by a hydrophobic residue—an exchange that is known to inactivate dipeptidase activity (25)—indicating that their metal center was inactivated in all these periplasmic PvdM homologs (Fig. 7, *right side*). Among these 41 periplasmic PvdM homologs, five belonged to the class of γ-proteobacteria, with members of the genera *Pantoea* (3x), *Cellvibrio*, and *Steroidobacter*, three belonged to the β-proteobacteria, all within the genus *Duganella*, and 33 came from α-proteobacterial genera *Sphingomonas* (11×), *Rhizorhabdus* (5×), *Caulobacter* (11×), *Sphingobium* (2×), *Novosphingobium* (2×), *Amphiplicatus* (1×), and *Glycocaulis* (1×). A phylogenetic tree based on the amino acid sequences of these PvdM homologs indicated a clustering that tightly correlated with the systematic position of these strains, with the exception of the PvdM homolog of *Steroidobacter*, which clustered together with PvdM homologs of *Sphingomonas* and *Rhizorhabdus* (Fig. 7). This could readily be understood when the functional associations were analyzed, as the PvdM homolog in *Steroidobacter* was associated with the same type of periplasmic

FAD-dependent oxidoreductase as the similar PvdM homologs of *Sphingomonas* and *Rhizorhabdus*. This is a strong evidence for an evolutionary adaptation of PvdM homologs to functionally associated FAD-dependent oxidoreductases. This functional association is even further supported by the fact that the two genes are most likely translationally coupled in the case of *Sphingomonas leidyi* and *Sphingomonas kyeonggiensis*, in which in a GTGA sequence, the translational start of the FAD-containing oxidoreductase gene overlaps with the translational stop of the *pvdM*-homologous gene. In other cases of this cluster, the stop and start codons are separated by only two bases.

Also, in several *Caulobacter* strains, an association with FAD-dependent oxidoreductases was observed. The FAD-containing oxidoreductases in *Caulobacter*, as the ones in *Sphingomonas*, *Rhizorhabdus*, and *Steroidobacter*, all contained twin-arginine motifs in N-terminal signal peptides, and TatFind (31) as well as SignalP (19) clearly predicted them to be Tat substrates. It therefore can be assumed that these flavoproteins need to assemble their FAD cofactor prior to transport into the periplasm (32). A functional interaction of these periplasmic oxidoreductases with their associated PvdM homologs might be similar as in the case of PvdM and PvdP in pyoverdine-producing bacteria. The FAD-dependent oxidoreductases belong to the family of glycine oxidases/D-amino acid oxidases, and it may thus well be that they are needed for the metabolism of D-amino acid–containing peptides in the periplasm, and the PvdM homologs may thus again serve to channel D-amino acid–containing peptides to an enzyme, as in the case of the PvdM–PvdP couple. PvdM homologs also occur in other genetic contexts that related to other biomolecules (Fig. 7). It can thus be expected that future studies will surely reveal functions of PvdM homologs in other pathways.

We also noted that the genes for the PvdM homologs were almost always in close proximity to genes encoding TonB-dependent receptors (Fig. 7). In the case of *Sphigomonas colocasiae* JCM31229, the two genes were overlapping by 20

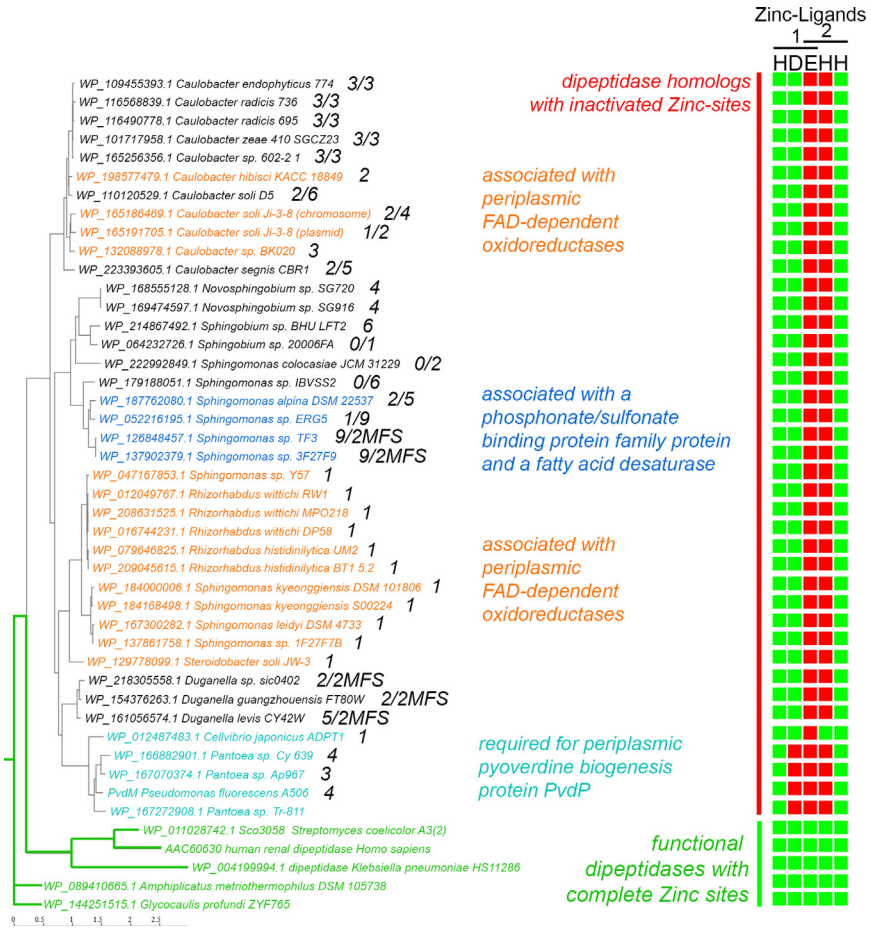

Figure 7. Periplasmic PvdM homologs occur in α-, β-, and γ-proteobacteria, genetically linked to uptake systems for biomolecules and diverse metabolic pathways. (*Left*) Phylogenetic tree, based on sequences of periplasmic PvdM homologs, in addition including the sequences of PvdM from *Pseudomonas fluorescens* A506, as well as the three dipeptidases Sco3058, human renal dipeptidase, and *Klebsiella pneumoniae* dipeptidase for comparison. Accession numbers are given for all sequences. The tree was generated using NGPhylogeny.fr (46). Parts of the tree with functional dipeptidases are in *green*. Functional associations are highlighted in other colors. Larger numbers behind strain names indicate the number(s) of genes separating the *pvdM* homologs from the next TonB-dependent receptor(s). Also, numbers of genes that separate *pvdM* homologs from MFS transporters are indicated (labeled MFS). Note that often two TonB-dependent receptors or both, a TonB-dependent receptor and an MFS-family transporter, are encoded nearby. (*Right*) Indication of the conservation of the five Zn^{2+} ligands from hrDP in the PvdM homologs analyzed in the phylogenetic tree (H, D, E, H, and H correspond to His-20, Asp-22, Glu-125, His-198, and His-219 of human renal dipeptidase). Colors indicate the presence (*green*) or the absence (*red*) of the respective ligand. hrDP, human renal dipeptidase; MFS, major facilitator superfamily.

codons. The only case of no direct association was a pyoverdine-producing strain that encoded its TonB-dependent pyoverdine uptake system elsewhere in the genome. In case of pyoverdine, TonB-dependent receptors are required for the uptake of ferric iron–loaded pyoverdines (10). It therefore can be said that all detected periplasmic PvdM homologs were associated with TonB-dependent uptake systems, suggesting that uptake of compounds is functionally related to the PvdM homologs. In addition to TonB-dependent receptors, also several genetic associations to major facilitator superfamily transporters were recognized (Fig. 7). It is thus possible that, similar to the case of pyoverdine, PvdM homologs are involved in pathways that include secretion and uptake of so far unknown biomolecules that may well be other siderophores.

The γ-proteobacteria of the genera *Pantoea* and *Cellvibrio* contained PvdM homologs very similar to PvdM from *Pseudomonas*. The genetic context of the *pvdM* genes revealed the presence of the pyoverdine biosynthesis genes in these strains, and the *pvdP* gene was in direct vicinity to *pvdM*, suggesting that pyoverdine-like siderophores are produced in these strains of Enterobacteriaceae (*Pantoea*) and Cellvibrionaceae (*Cellvibrio*). Therefore, PvdM homologs in these γ-proteobacteria likely function as they do in fluorescent pseudomonads (Fig. 7).

Discussion

PvdM has been the last protein of unknown function that is known to be essential for pyoverdine biogenesis. In most pseudomonads, PvdM is encoded in the *pvdMNO* operon in which *pvdM* is the only gene that is truly essential for pyoverdine biogenesis, as shown by scarless in-frame deletion with *P. fluorescens* A506 as model organism (13). The other two genes in this operon encode enzymes for conversion of the N-terminal glutamate to succinamide (PvdN, 11) and for the last oxidation step during fluorophore formation (PvdO, 13). The essential role of PvdM has been puzzling, as all enzymatic biosynthesis steps had already been attributed to other proteins. Since PvdM belongs to a family of functional dipeptidases, including hrDP and bacterial dipeptidases, people assumed that PvdM has some dipeptidase function, and consequently, PvdM homologs have been generally assigned as "dipeptidase" in genome analyses.

To develop ideas for the potential function of PvdM, we first needed to know whether PvdM is cytoplasmic or periplasmic. Our biochemical analyses clearly demonstrated that PvdM is a periplasmic protein that is anchored to the cytoplasmic membrane by a single N-terminal transmembrane domain and a second so far not identified membrane anchor (Figs. 1 and 2). Based on this finding and on the assumption that PvdM might be a peptidase, a plausible scenario was that PvdM is the so-far unknown peptidase that is required for the initial step of the inactivation of the antisigma factor FpvR, which is the basis for the activation of the sigma factors PvdS and FpvI that regulate pyoverdine biosynthesis (10). However, our analysis of this potential role clearly showed that PvdM did not have this function (Fig. 3).

We thus searched for further possible functions of PvdM. To test whether PvdM might be involved in the periplasmic pyoverdine maturation pathway, which requires deacylation of ferribactin (PvdQ) and fluorophore formation (PvdP and PvdO), we analyzed potential biogenesis intermediates that are formed in the *ΔpvdM* mutant strain by mass spectrometry and found that deacylated ferribactin, the substrate of PvdP (27), is secreted into the medium (Fig. 4). Therefore, PvdM is required to prevent secretion of ferribactin, and as PvdP apparently cannot access ferribactin as substrate without PvdM *in vivo*, PvdM somehow ensures the delivery of ferribactin to PvdP. While there are several scenarios possible, we think the most likely one is a direct transfer of ferribactin to PvdP by PvdM. An obligate transfer would explain best that no detectable pyoverdine was formed without PvdM, and PvdM contains a peptide-binding site–like renal dipeptidase that is known to bind peptides with D- and L-amino acids, and ferribactin contains D- and L-amino acids. Based on our findings, we now can integrate PvdM into the periplasmic pyoverdine maturation pathway (Fig. 8).

It has been shown that purified PvdP does not require any other protein for function (27, 28). It is therefore crucial to understand, why PvdM is integrated into the biosynthetic pathway. To answer this, it is important to take the secretion of deacylated ferribactin by the *ΔpvdM* mutant strain into account. It is clear that, without PvdM, the biosynthetic intermediate ferribactin cannot be kept inside the cells. The secretion systems that can secrete pyoverdines are thus insufficiently specific to discriminate ferribactin from mature pyoverdines. Recent studies on pyoverdine secretion in *Pseudomonas putida* have provided evidence for the involvement of at least three secretion systems in pyoverdine secretion (33). It is clear that the PvdRT-OpmQ secretion system, which is encoded in conjunction with pyoverdine biosynthesis genes, is the most important one. However, also the multidrug-efflux resistance–nodulation–division transporter MdtABC-OpmB and at least one unknown system transport pyoverdines (33). These systems are widespread among pseudomonads. In *P. fluorescens*, the MdtABC-OpmB system is encoded in the genes PflA506 2944-PflA506 2947, and in *P. aeruginosa*, the homologous system is encoded in the genes PA2525–PA2528. The specificity for ferribactin has never been tested for any of these transporters, but at least in case of the multidrug-efflux resistance–nodulation–division transporters, it can be expected that they contribute to the secretion of biosynthesis intermediates, if they are freely diffusing in the periplasm. PvdM therefore prevents free diffusion of ferribactin in the periplasm, thereby blocking premature export of biosynthesis intermediates. This is a similar function as that of binding proteins that capture periplasmic compounds to enable their import into the cytoplasm by ABC transporter–dependent uptake systems (34). However, although binding proteins are known that serve to bring peptides of up to 18 residues in length to their corresponding transporter, such binding proteins serve in peptide scavenging and thus have little sequence specificity. A closer look at the structure of PvdM reveals that the region of the renal dipeptidase peptide–binding site is

conserved, including residues important for cilastatin binding (Fig. 6*A*). An additional lobe that is not found in the dipeptidases but present in PvdM homologs might constitute additional binding surfaces to increase substrate specificity or binding affinity. Alternatively, this lobe could function as a clamp for chaperone-like reversible binding and release of substrates, which are interesting biochemical aspects that need to be clarified in future.

Our finding that PvdM homologs occur not only associated with PvdP and thus pyoverdine biogenesis but also with FAD-dependent oxidases of the D-amino acid oxidase family and other proteins suggests that PvdM is not limited to pyoverdine biosynthesis but can exert its function also for other D-amino acid–containing peptides or other specific biomolecules inside the periplasm. This opens a new field for research, as many pathways with unknown enzymes and substrates remain to be discovered.

Experimental procedures

Strains and growth conditions

E. coli DH5α (Invitrogen) and XL1-Blue (Agilent) were used for cloning, and *P. fluorescens* A506 (kindly provided by Joyce E. Loper) and *E. coli* BL21 (DE3) (Agilent) were used for functional or biochemical analyses. *P. fluorescens* and *E. coli* strains were aerobically grown at 30 and 37 °C, respectively, in LB medium, M9 medium, or CAA medium, as indicated. When required, the medium was supplemented with appropriate antibiotics (ampicillin, 100 μg/ml; chloramphenicol, 25 μg/ml; and kanamycin, 50 μg/ml). For strict iron depletion, media were supplemented with 0.5 mg/ml EDDHA.

Complementation analyses and growth curves

For complementation analysis, cells corresponding to 1 ml absorbance of 1 at 600 nm of an overnight culture in CAA medium were washed three times in 1 ml saline (0.9% [w/v] NaCl) solution. The final pellet was resuspended in 1 ml saline solution, and 10 μl droplets were placed on CAA media plates.

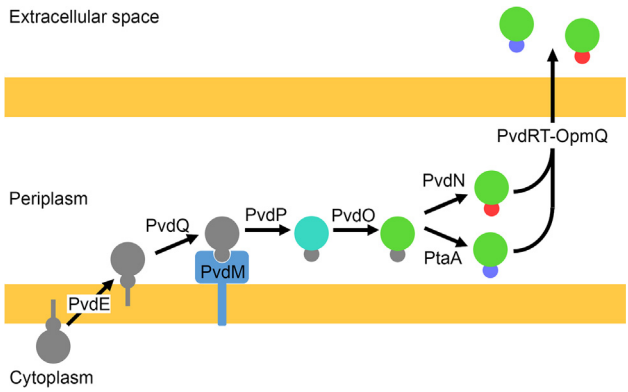

Figure 8. Model for the integration of PvdM in the periplasmic pyoverdine maturation steps. Ferribactin is transported by PvdE and deacylated by PvdQ. PvdM binds deacylated ferribactin, thereby preventing its secretion, and delivers it to PvdP that initiates fluorophore formation, which is completed by PvdO. PvdN and PtaA modify the N-terminal glutamic acid to succinamide (*red*) or α-ketoglutarate (*blue*), before the pyoverdine is secreted into the extracellular space.

Growth and pyoverdine production were examined after 36 h at 30 °C.

Growth curves were recorded using a SpectraMaxiD3 microplate reader (Molecular Devices), with absorbance at 600 nm measurements every 15 min. Wells containing 198 μl medium were inoculated with 2 μl of washed overnight cultures that had been normalized to an absorbance of 1 at 600 nm.

Genetic methods and plasmids

The coding region of *pvdM*, including a C-terminal *Strep*-tag used for later Western blot detections, was amplified from the plasmid pEXPT7-*pvdM*-strep (13) by PCR with the primer pair *SpeI*-RBS-*PvdM*-F-MS and pEXPT7-Strep-term-R-MS (see Table 1 for primers) and subcloned into pUCP20-ANT2-MCS (35), using SpeI/HindIII restriction sites, resulting in the plasmid pUCP20-ANT2-*pvdM*-strep-term for expression in *P. fluorescens*, and into pEXH5-*tac* (36) using NdeI/HindIII restriction sites, resulting in the plasmid pEX-*pvdM*-strep-term-tac for expression in *E. coli*. Single amino acid exchanges in the globular domain of PvdM were introduced by QuikChange mutagenesis (Stratagene) of pUCP20-ANT2-*pvdM*-strep-term, using the primers *pvdM*-M246A-F-MS or *pvdM*-H266A-F-MS in conjunction with the reverse primers that cover the identical sequence region, resulting in pUCP20-ANT2-*pvdM*M246A-strep-term and pUCP20-ANT2-*pvdM*H266A-strep-term. The ASA cleavage site was introduced *via* a gene synthesis, as QuikChange turned out to be not suitable for this specific very GC-rich (70%) region. For the fusion of the complete signal peptide of PvdO to the mature domain of PvdM, DNA encoding these domains was amplified by PCR using the primers KpnI-RBS-*pvdO*-F-MS, *pvdO*-SP-R-MS, mat-*pvdM*-F-MS, pEXPT7-Strep-term-R-MS, and cloned in the corresponding sites of pUCP20-ANT2, resulting in pUCP20-ANT2-SP-*pvdO*-mat-*pvdM*-strep-term. For insertion of a hexahistidine tag at the N-terminus of the signal peptide of PvdM and PvdO, which was only used for early experiments that are not part of this study, the respective fragments encoding the domains were amplified by PCR using the primers His-SP-*pvdM*-for-MS, His-SP-*pvdO*-F-2-MS, and pEXPT7-Strep-term-R-MS, resulting in pUCP20-ANT2-His-*pvdM*-strep-term, pUCP20-ANT2-His-*pvdM*-ASA-strep-term, and pUCP20-ANT2-His-SP-*pvdO*-mat-*pvdM*-strep-term. Note that the N-terminal hexahistidine tag did not interfere with membrane targeting and functionality. For the exchange of the signal peptide of PhoA with that of PvdM and PvdO, the DNA fragments encoding these domains were amplified by PCR using the primers His-SP-*pvdM*-F-MS, SP-*pvdM*-mat-*pvdO*-R-MS, SP-*pvdM*-mat-*pvdO*-F-MS, pEXPT7-Strep-term-R-MS, SP*pvdO*-mat*phoA*-R-MS, SP*pvdO*-mat-*phoA*-F-MS, SP-*pvdM*-mat-*phoA*-R-MS, mat-*phoA*-F-MS, and mat-*phoA*-strep-MfeI-R-MS and cloned in the corresponding sites of pUCP20-ANT2-MCS, resulting in pUCP20-ANT2-His-SP-*pvdM*-mat-*phoA*-strep-term, pUCP20-ANT2-His-SP-*pvdO*-mat-*phoA*-strep-term, pUCP20-ANT2-*phoA*-strep-term, and pUCP20-ANT2-mat-*phoA*-strep-term.

Extraction of pyoverdines or biosynthetic precursors

Pyoverdines or precursors were extracted based on the method by Meyer *et al.* (37). Briefly, 1 ml of an overnight culture (in CAA medium) was used to inoculate 1 l CAA medium. The culture was grown for 72 h (30 °C, 180 rpm), cells were sedimented (30′, 20,000*g*, 4 °C; Sorvall Lynx 4000 centrifuge; Thermo Fisher Scientific), and the supernatant was sterile filtered (0.2 μm pore size) using the Filtropur V50 system (Sarstedt, Inc). The pH was adjusted to 6.0 using 8 M HCl, and 20 g/l XAD-4 resin was added. After 3 h incubation at 4 °C, the resin was filtered, the flow through was discarded, and the resin was resuspended in 0.5 l H_2O. After another incubation for 1 h at 4 °C, the resin was filtered, resuspended in 200 ml 15% methanol, incubated for 15 min at 4°, and filtered again. Then, the resin was resuspended in 150 ml 50% methanol, incubated for 1 h at 4°, and filtered. The solvent was removed using a rotary evaporator, kept at 30 °C (Rotavapor R-124), and the pyoverdine or its biosynthetic intermediates were resuspended in 1 ml H_2O and filtered (Filtropur S filter; Sarstedt, Inc).

Biochemical and analytical methods

Subcellular fractionations into periplasm, membranes, and cytoplasm were based on an established protocol (38) with minor modifications. Briefly, a cell pellet corresponding to 100 ml absorbance of 1 at 600 nm of an overnight culture was washed with 1 ml 50 mM Tris–HCl (pH 7.6) and resuspended in 1 ml of 200 mM $MgCl_2$ and 50 mM Tris–HCl (pH 7.6). The suspension was incubated for 30 min at 30 °C and 300 rpm and cooled on ice for 5 min. After a final incubation for 15 min at room temperature, the cells were centrifuged for 10 min at 8,000*g*. A sample was taken from the supernatant and kept as periplasmic fraction. The cells were washed in 1 ml of 50 mM Tris–HCl (pH 7.6), harvested by centrifugation for 10 min at 8,000*g* at 4 °C, and resuspended in 1 ml of 50 mM Tris–HCl (pH 7.6). The suspension was sonicated three times and centrifuged for 15 min at 13,000*g* to remove cell debris. The supernatant was ultracentrifuged for 45 min at 120,000*g* at 4 °C. The supernatant was collected as the cytoplasmic fraction, and the resulting pellet was resuspended in 50 mM Tris–HCl (pH 7.6) and kept as membrane fraction.

SDS-gels and Western blots were performed using standard protocols (39–41). The *Strep*-tag and the BCCP were detected by horseradish peroxidase–coupled Strep-Tactin (IBA).

For protease accessibility assays, a cell pellet corresponding to 100 ml absorbance of 1 at 600 nm was resuspended in 2.5 ml 33 mM Tris–HCl (pH 8.0), 40% sucrose, and 5 mM Na_2EDTA and incubated for 30 min at 4 °C. The suspension was centrifuged for 15 min at 7000*g*, and the cells were resuspended in 1 ml 33 mM Tris–HCl (pH 8.0) and 40% sucrose at 4 °C. About 200 μl of these outer membrane–permeabilized cells were then incubated for 30 min at 25 °C in the presence of 0.5 mg/ml proteinase K with or without 2% (v/v) Triton X-100, respectively (21).

The PhoA assay was carried out according to Ref. (42). Briefly, 5 ml of LB medium was inoculated with 125 μl of an overnight culture and grown to an absorbance 0.8 to 1.0 at 600 nm. Cells were then cooled on ice for 20 min, and 500 μl were centrifuged at 13,000*g* for 10 min. The obtained pellet was resuspended in 2 ml 1 M Tris–HCl (pH 8.0). While 1 ml was used to determine the absorbance at 600 nm, the remaining 1 ml suspension was mixed with 100 μl *p*-nitrophenyl phosphate solution [0.4% *p*-nitrophenyl phosphate in 1 M Tris–HCl (pH 8.0)] as substrate and incubated at room temperature. The reaction was stopped by adding 100 μl 1 M K_2HPO_4 when a yellow coloring became visible but after 10 min at the latest. The reaction mix was centrifuged for 2 min at 13,000*g*, and the absorbance of the supernatant was determined at 420 nm and used for the calculation of the activity according to Ref. (42).

For detection of fluorescent pyoverdine in liquid samples, absorbance spectra were recorded using the DS-11 UV–Vis Spectrophotometer (DeNovix). Detection and identification of ferribactin and pyoverdines *via* LC–MS was carried out as described previously (11).

Table 1
Primers used in this study

Primers	Sequence (5'>3')
Primers for expression vectors (non-mutated)	
SpeI-RBS-PvdM-F-MS	CTTGACTAGTGTTTAACTTTAAGAAGGAGATATACATATGACAAAATCACGTTCG
pEXPT7-Strep-term-R-MS	CCCTAAGCTTGAATTCAAAAAAAACCCCGCCCTGTCAGGGGCGGGG TTTTTTTTTTCAT TACTTTTCGAACTGCGGGTGGCTCC
KpnI-RBS-*pvdO*-F-MS	CTTGGGTACCGTTTAACTTTAAGAAGGAGATATACATATGACGCCATCCCGACTCAAAC
pvdO-SP-R-MS	CCAGCAAGCCGGCATGGGCCAGGCCGGGC
mat-*pvdM*-F-MS	CGCAAGCTTTTACTTTTCGAACTGCGGGTGGCTCCAGC
His-SP-*pvdM*-F-MS	GATATACATATGACACACCATCACCATCACCATAAATCACGTTCGAAAAAGGCGCTG
His-SP-*pvdO*-F-2-MS	GATATACATATGACGCACCATCACCATCACCATCCATCCCGACTCAAACCGCTCACCG
SP*pvdM*-mat-*pvdO*-R-MS	GTGGGGCGGCCAGCAAGCCAGCCCCGGCG
SP*pvdM*-mat-*pvdO*-F-MS	GCTGGCTTGCTGGCCGCCCCACAACCGGGCAAGG
SP*pvdO*-mat-*phoA*-R-MS	GGTGTCCGGGCATGGGCCAGGCCGGGCAGCAGGGCGCCGCACAGGGC
SP*pvdO*-mat-*phoA*-F-MS	GGCCCATGCCCGGACACCAGAAATGCCTGTTCTGG
SP*pvdM*-mat-*phoA*-R-MS	CTGGTGTCCGCAGCAAGCCAGCCCCGGCGCCG
mat-*phoA*-F-MS	GCTGGCTTGCTGCGGACACCAGAAATGCCTG
mat-*phoA*-strep-MfeI-R-MS	GAGCAATTGTTACTTTTCGAACTGCGGGTGGCTCCATTTCAGCCCCAGAGCGGC
Primers for amino acid exchanges[a]	
pvdM-M246A-F-MS	CGTGTCGCAGGCGTCGACCAAGG
pvdM-H266A-F-MS	GGTGGCGTCCGCCTCGGCGCCTC

[a] Corresponding reverse primers covered the same sequence.

Data availability

All data are contained within the article.

Supporting information—This article contains supporting information.

Acknowledgments—We gratefully acknowledge the skillful technical assistance of Sybille Traupe, Katrin Gunka, and Inge Reupke (Leibniz University Hannover).

Author contributions—T. B. conceptualization; M.-F. S. and M. T. R. methodology; M.-F. S. validation; M.-F. S., A. N. B., G. D., and T. B. investigation; T. B. writing–original draft; M.-F. S., A. N. B., M. T. R., G. D., and T. B. writing–review & editing; M.-F. S. and T. B. visualization; T. B. supervision; T. B. funding acquisition.

Funding and additional information—This work was supported by grant BR 2285/7-1 of the German Research Foundation (DFG) to T. B.

Conflict of interest—The authors declare that they have no conflicts of interest with the contents of this article.

Abbreviations—The abbreviations used are: BCCP, biotin carboxyl carrier protein; CAA, casamino acid; EDDHA, ethylene diamine-*N*,*N*′-bis(2-hydroxyphenylacetic acid); hrDP, human renal dipeptidase; PhoA, alkaline phosphatase.

References

1. Marelja, Z., Leimkühler, S., and Missirlis, F. (2018) Iron sulfur and Molybdenum cofactor enzymes regulate the Drosophila life cycle by controlling cell metabolism. *Front. Physiol.* **9**, 50
2. Berrisford, J. M., Baradaran, R., and Sazanov, L. A. (2016) Structure of bacterial respiratory complex I. *Biochim. Biophys. Acta* **1857**, 892–901
3. Cunningham, R. P., Asahara, H., Bank, J. F., Scholes, C. P., Salerno, J. C., Surerus, K., *et al.* (1989) Endonuclease III is an iron-sulfur protein. *Biochemistry* **28**, 4450–4455
4. Romero, A. M., Martínez-Pastor, M. T., and Puig, S. (2021) Iron in translation: from the beginning to the end. *Microorganisms* **9**, 1058
5. Stefánsson, A. (2007) Iron (III) hydrolysis and solubility at 25 degrees C. *Environ. Sci. Technol.* **41**, 6117–6123
6. Chu, B. C., Garcia-Herrero, A., Johanson, T. H., Krewulak, K. D., Lau, C. K., Peacock, R. S., *et al.* (2010) Siderophore uptake in bacteria and the battle for iron with the host; a bird's eye view. *Biometals* **23**, 601–611
7. Vansuyt, G., Robin, A., Briat, J.-F., Curie, C., and Lemanceau, P. (2007) Iron acquisition from Fe-pyoverdine by Arabidopsis thaliana. *Mol. Plant Microbe Interact.* **20**, 441–447
8. Lamont, I. L., Beare, P. A., Ochsner, U., Vasil, A. I., and Vasil, M. L. (2002) Siderophore-mediated signaling regulates virulence factor production in *Pseudomonas aeruginosa*. *Proc. Natl. Acad. Sci. U. S. A.* **99**, 7072–7077
9. Wendenbaum, S., Demange, P., Dell, A., Meyer, J. M., and Abdallah, M. A. (1983) The structure of pyoverdine Pa, the siderophore of Pseudomonas aeruginosa. *Tetrahedron Lett.* **24**, 4877–4880
10. Ringel, M. T., and Brüser, T. (2018) The biosynthesis of pyoverdines. *Microb. Cel. (Graz, Austria)* **5**, 424–437
11. Ringel, M. T., Dräger, G., and Brüser, T. (2016) PvdN enzyme catalyzes a periplasmic pyoverdine modification. *J. Biol. Chem.* **291**, 23929–23938
12. Ringel, M. T., Dräger, G., and Brüser, T. (2017) The periplasmic transaminase PtaA of Pseudomonas fluorescens converts the glutamic acid residue at the pyoverdine fluorophore to α-ketoglutaric acid. *J. Biol. Chem.* **292**, 18660–18671
13. Ringel, M. T., Dräger, G., and Brüser, T. (2018) PvdO is required for the oxidation of dihydropyoverdine as the last step of fluorophore formation in Pseudomonas fluorescens. *J. Biol. Chem.* **293**, 2330–2341
14. Nitanai, Y., Satow, Y., Adachi, H., and Tsujimoto, M. (2002) Crystal structure of human renal dipeptidase involved in β-Lactam hydrolysis. *J. Mol. Biol.* **321**, 177–184
15. Blum, M., Chang, H.-Y., Chuguransky, S., Grego, T., Kandasaamy, S., Mitchell, A., *et al.* (2021) The InterPro protein families and domains database: 20 years on. *Nucl. Acids Res.* **49**, D344–D354
16. Winsor, G. L., Griffiths, E. J., Lo, R., Dhillon, B. K., Shay, J. A., and Brinkman, F. S. L. (2016) Enhanced annotations and features for comparing thousands of *Pseudomonas* genomes in the Pseudomonas genome database. *Nucl. Acids Res.* **44**, D646–D653
17. Braun, P., and von Heijne, G. (1999) The aromatic residues Trp and Phe have different effects on the positioning of a transmembrane helix in the microsomal membrane. *Biochemistry* **38**, 9778–9782
18. Adachi, H., Katayama, T., Inuzuka, C., Oikawa, S., Tsujimoto, M., and Nakazato, H. (1990) Identification of membrane anchoring site of human renal dipeptidase and construction and expression of a cDNA for its secretory form. *J. Biol. Chem.* **265**, 15341–15345
19. Petersen, T. N., Brunak, S., von Heijne, G., and Nielsen, H. (2011) SignalP 4.0: discriminating signal peptides from transmembrane regions. *Nat. Met.* **8**, 785–786
20. Hoffman, C. S., and Wright, A. (1985) Fusions of secreted proteins to alkaline phosphatase: an approach for studying protein secretion. *Proc. Natl. Acad. Sci. U. S. A.* **82**, 5107–5111
21. Porcelli, I., Leeuw, E. de, Wallis, R., van den Brink-van der Laan, E., Kruijff, B. de, Wallace, B. A., *et al.* (2002) Characterization and membrane assembly of the TatA component of the Escherichia coli twin-arginine protein transport system. *Biochemistry* **41**, 13690–13697
22. Draper, R. C., Martin, L. W., Beare, P. A., and Lamont, I. L. (2011) Differential proteolysis of sigma regulators controls cell-surface signalling in Pseudomonas aeruginosa. *Mol. Microbiol.* **82**, 1444–1453
23. Cummings, J. A., Nguyen, T. T., Fedorov, A. A., Kolb, P., Xu, C., Fedorov, E. V., *et al.* (2010) Structure, mechanism, and substrate profile for Sco3058: the closest bacterial homologue to human renal dipeptidase. *Biochemistry* **49**, 611–622
24. Keynan, S., Hooper, N. M., and Turner, A. J. (1997) Identification by site-directed mutagenesis of three essential histidine residues in membrane dipeptidase, a novel mammalian zinc peptidase. *Biochem. J.* **326**, 47–51
25. Adachi, H., Katayama, T., Nakazato, H., and Tsujimoto, M. (1993) Importance of Glu-125 in the catalytic activity of human renal dipeptidase. *Biochim. Biophys. Acta* **1163**, 42–48
26. Campbell, B. J., Di Yuan, S., Forrester, L. J., and Zahler, W. L. (1988) Specificity and inhibition studies of human renal dipeptidase. *Biochim. Biophys. Acta* **956**, 110–118
27. Nadal-Jimenez, P., Koch, G., Reis, C. R., Muntendam, R., Raj, H., Jeronimus-Stratingh, C. M., *et al.* (2014) PvdP is a tyrosinase that drives maturation of the pyoverdine chromophore in *Pseudomonas aeruginosa*. *J. Bacteriol.* **196**, 2681–2690
28. Poppe, J., Reichelt, J., and Blankenfeldt, W. (2018) Pseudomonas aeruginosa pyoverdine maturation enzyme PvdP has a noncanonical domain architecture and affords insight into a new subclass of tyrosinases. *J. Biol. Chem.* **293**, 14926–14936
29. McGinnis, S., and Madden, T. L. (2004) Blast: at the core of a powerful and diverse set of sequence analysis tools. *Nucl. Acids Res.* **32**, W20–W25
30. Sonnhammer, E. L., von Heijne, G., and Krogh, A. (1998) A hidden Markov model for predicting transmembrane helices in protein sequences. *Proc. Int. Conf. Intell. Syst. Mol. Biol.* **6**, 175–182
31. Rose, R. W., Brüser, T., Kissinger, J. C., and Pohlschröder, M. (2002) Adaptation of protein secretion to extremely high-salt conditions by extensive use of the twin-arginine translocation pathway. *Mol. Microbiol.* **45**, 943–950
32. Natale, P., Brüser, T., and Driessen, A. J. M. (2008) Sec- and Tat-mediated protein secretion across the bacterial cytoplasmic membrane–distinct translocases and mechanisms. *Biochim. Biophys. Acta* **1778**, 1735–1756

33. Henríquez, T., Stein, N. V., and Jung, H. (2019) PvdRT-OpmQ and MdtABC-OpmB efflux systems are involved in pyoverdine secretion in Pseudomonas putida KT2440. *Environ. Microbiol. Rep.* **11**, 98–106
34. Maqbool, A., Horler, R. S. P., Muller, A., Wilkinson, A. J., Wilson, K. S., and Thomas, G. H. (2015) The substrate-binding protein in bacterial ABC transporters: dissecting roles in the evolution of substrate specificity. *Biochem. Soc. Trans.* **43**, 1011–1017
35. Hoffmann, L., Sugue, M.-F., and Brüser, T. (2021) A tunable anthranilate-inducible gene expression system for Pseudomonas species. *Appl. Microbiol. Biotechnol.* **105**, 247–258
36. Richter, S., and Brüser, T. (2005) Targeting of unfolded PhoA to the TAT translocon of Escherichia coli. *J. Biol. Chem.* **280**, 42723–42730
37. Meyer, J. M., Stintzi, A., Vos, D. de, Cornelis, P., Tappe, R., Taraz, K., *et al.* (1997) Use of siderophores to type pseudomonads: the three *Pseudomonas aeruginosa* pyoverdine systems. *Microbiology* **143**, 35–43
38. Izé, B., Viarre, V., and Voulhoux, R. (2014) Cell fractionation. *Met. Mol. Biol.* **1149**, 185–191
39. Laemmli, U. K. (1970) Cleavage of structural proteins during the assembly of the head of bacteriophage T4. *Nature* **227**, 680–685
40. Burnette, W. (1981) "Western Blotting": electrophoretic transfer of proteins from sodium dodecyl sulfate-polyacrylamide gels to unmodified nitrocellulose and radiographic detection with antibody and radioiodinated protein A. *Anal. Biochem.* **112**, 195–203
41. Towbin, H., Staehelin, T., and Gordon, J. (1979) Electrophoretic transfer of proteins from polyacrylamide gels to nitrocellulose sheets: procedure and some applications. *Proc. Natl. Acad. Sci. U. S. A.* **76**, 4350–4354
42. Brickman, E., and Beckwith, J. (1975) Analysis of the regulation of Escherichia coli alkaline phosphatase synthesis using deletions and Φ80 transducing phages. *J. Mol. Biol.* **96**, 307–316
43. Crooks, G. E., Hon, G., Chandonia, J.-M., and Brenner, S. E. (2004) WebLogo: a sequence logo generator. *Genome Res.* **14**, 1188–1190
44. Arnold, K., Bordoli, L., Kopp, J., and Schwede, T. (2006) The SWISS-model workspace: a web-based environment for protein structure homology modelling. *Bioinformatics* **22**, 195–201
45. *The PyMOL Molecular Graphics System*. (2021), Schrödinger, New York, NY Version 2.5.2. https://pymol.org/2/support.html?
46. Lemoine, F., Correia, D., Lefort, V., Doppelt-Azeroual, O., Mareuil, F., Cohen-Boulakia, S., *et al.* (2019) NGPhylogeny.fr: New generation phylogenetic services for non-specialists. *Nucl. Acids Res.* **47**, W260–W265